

EXPERIMENTAL INVESTIGATION OF COMPOSITE PATCH REINFORCED CORRODED STEEL PLATES IN STATIC LOADING

Nicholas G. Tsouvalis, Lazarus S. Mirisiotis and Theodora E. Tsiourva

Shipbuilding Technology Laboratory, School of Naval Architecture and Marine Engineering,
National Technical University of Athens, GR-15773 Zografos, Athens, Greece
tsouv@mail.ntua.gr

ABSTRACT

This paper is an experimental investigation of the efficiency of a carbon/epoxy composite patch for reinforcing a steel plate with a large artificially corroded area. The thickness loss of the steel plate after 200 cycles of accelerated cyclic corrosion exposure was equal to approximately 15%. Patches were laminated on one-side of the steel plate using either the hand lay-up or the vacuum infusion method. Common, low cost composite materials were used for the patches, in an effort to assess the effectiveness of a reinforcement that could be executed in situ in the harsh marine environment of a ship by properly trained personnel. In addition, an advanced high modulus unidirectional carbon fabric was used, raising the number of different patches tested to three. The surface preparation of the steel specimens was simple and quick. Strains were monitored at several locations both on the patch and on the steel substrate. In all cases first failure appeared as patch debonding, either sudden or progressive. Despite the low stiffness ratio of the patch reinforcements, experimental measurements indicated that the maximum load reached by the patched specimens before patch debonding was increased with respect to the yield load of the reference unpatched specimens by 13 to 28%.

1. INTRODUCTION

Although composite patches have been extensively used for repairing or reinforcing aluminum aircraft structures, their applications to steel marine structures are until now very few. The various defect types met in steel marine structures and the nature of their loading reveal often the need for local reinforcements or repairs, with the aim of either increasing the residual strength of the structure or elongating its operational life in cyclic loading. Composite material patches are a very attractive solution for these reinforcements or repairs, overcoming several significant drawbacks induced by the conventional repair methods. Hence, composite patches can be successfully used in areas with complicated geometry, or where the use of hot and sparking work like welding, is either quite costly or prohibitive (i.e. in structures under permanent tension or in fuel cargo holds or tanks).

Although the literature concerning aluminum aircraft applications of composite patch reinforcements is quite extended (i.e. [1-3]), there are very few reported works about composite patch applications in steel marine structures. These works concern composite patch reinforcements of secondary structural parts of some navy ships initially applied in the '80s, which have been extended lately to FPSOs (Floating Production Storage and Offloading vessels) [4-7]. The aim of this paper is to investigate through experiments the efficiency of a composite patch for reinforcing a steel plate with a large artificially corroded area that is loaded in static tension. Large scale specimens with a central corroded area were tested, reinforced on their corroded side by a carbon/epoxy composite patch. Two methods were used for manufacturing the composite patches, namely common hand lay-up and vacuum infusion, in combination with two carbon fabrics. Corroded plates were tested as one of the three

defected plate cases that were investigated within the framework of the same experimental program [8-10].

2. EXPERIMENTAL PROCEDURE

2.1 Materials

Normal grade A steel plates were used for the test specimens, whose experimentally derived tensile properties were 200 GPa for the Young's modulus and 348 MPa for the yield stress. Two different types of carbon fabric were used for the composite patches. The first type was a 160 g/m², 0°/90°, Twill 2x2 fabric from R&G Faserverbundwerkstoffe GmbH (T). The second type was a 300 g/m² unidirectional fabric with high modulus fibers from SIKA and code name SikaWrap – 300C HiMod NW (UD-HM). Two methods were used for manufacturing the composite laminated patches, namely the hand lay-up (HLU) and the vacuum infusion (VI). Patches with the Twill fabric were manufactured using both methods, whereas patches with the unidirectional SikaWrap fabric were manufactured using only the HLU method.

Each carbon fabric type was used in combination with a different type of resin. The first type, used with the Twill fabric, was D.E.R. 358 low viscosity epoxy resin from DOW (viscosity equal to 600–750 mPa·s at 25°C). Patches with this fibre/resin combination were made using both HLU and VI method. The second resin type was exclusively used in combination with the SikaWrap fabric and the HLU method and is Sikadur 300 epoxy resin from SIKA.

Before the initiation of the composite patched steel specimens' experimental program, a material characterization of the composite materials used for manufacturing all patches had been performed, for all combinations of materials and manufacturing methods. The results of these tests are summarized in [11].

2.2 Geometry of specimens

Figure 1 presents the geometry and main dimensions of the specimens. The nominal thickness of the steel plates is 4 mm. The central orthogonal part of the specimen has a length of 400 mm and a width of 140 mm. A central orthogonal part having length 160 mm and width 140 mm on one side of the specimen (front side) was subjected to corrosion, by putting the properly partially covered specimens in a special salt spray chamber. The corroded area was then

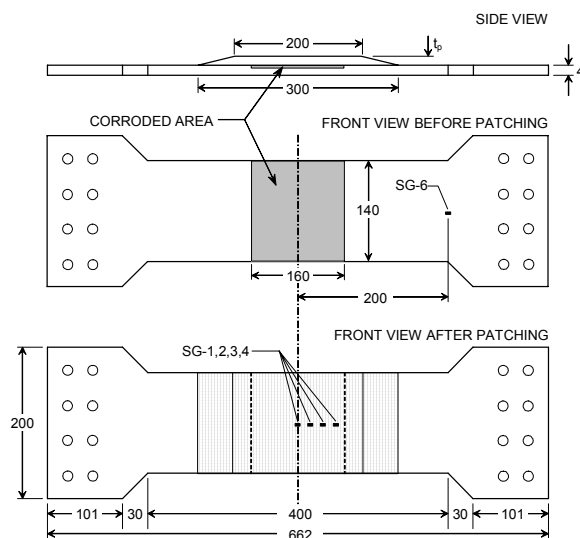


Figure 1: Specimen geometry.

covered by a central composite patch of thickness t_p , effective length 200 mm and width 140 mm. The total patch length is greater, equal to 300 mm, since it additionally includes the tapered edges of the patch (see Figure 1).

Four different couples of identical specimens were tested, corresponding to different patch material and manufacturing method. The terminology of the specimens, their basic characteristics and the exact width and thickness of the steel central orthogonal part before and after corrosion are listed in

Table 1. The thicknesses values before and after corrosion listed in the table are the average of three different corresponding measurements.

Table 1: Specimens' terminology and basic dimensions.

Specimen	Patch Material	Manufacturing Method	Width (mm)	Thickness before corrosion (mm)	Thickness after corrosion (mm)
S-COR-1	–	–	139.8	3.9	3.3
S-COR-2	–	–	140.2	3.8	3.2
S-COR-HLU-1	T	HLU	139.8	3.8	3.1
S-COR-HLU-2	T	HLU	139.8	3.7	3.3
S-COR-VI-1	T	VI	139.8	3.8	3.3
S-COR-VI-2	T	VI	140.7	3.7	3.2
S-COR-HLU-3	UD-HM	HLU	139.9	3.9	3.5
S-COR-HLU-4	UD-HM	HLU	140.0	3.8	3.3

2.3 Preparation and manufacturing of specimens

The area intended to be corroded was first marked and a simple electric rotating wire brush was then used to remove the existing primer. In the sequence, the area was cleaned by acetone and its thickness was measured, resulting in the values listed in Table 1. Then, the rest of the specimen was covered by a special nylon sheet. The only exposed area of the specimen was the one intended to be corroded, on one of its sides.

The accelerated cyclic corrosion testing was performed according to ISO 14993:2001 standard. A salt spray chamber was used in order to apply the standard. The solution used in the chamber was NaCl 3.5%, which corresponds to the typical NaCl concentration of sea water. Details for the chamber used and the accelerated corrosion procedure followed can be found in [11]. The specimens were subjected to cyclic conditions of accelerated corrosion for 70 days (approximately 200 corrosion cycles). Figure 2 shows a close view of the corroded area of a specimen, just after its removal from the chamber. Cleaning of the specimens and removal of corrosion products was done in accordance with the requirements of standard ISO 8407:1991.

All composite patches were laminated and cured directly on each steel specimen.



Figure 2: Specimen S-COR-VI-1 after its removal from the salt spray chamber.

Figure 3 shows an intermediate stage of the vacuum infusion procedure of the patches of specimens S-COR-VI-1 & 2. The number of layers and, hence, the patch thickness, t_p , were defined on the basis of a desired value for the stiffness ratio (SR), according to the equation $t_p = (SR \cdot t_s \cdot E_s) / E_p$, where t_p and E_p are the patch thickness and Young's modulus, respectively, and t_s and E_s are the steel plate thickness and Young's modulus.

With reference to patches made of Twill 2x2 fabric, its relatively low tensile modulus (41500 MPa) compared to that of steel (200000 MPa), led to the calculation of an unacceptably high t_p value for normal values of SR. Therefore, in order to manufacture patches



Figure 3: Vacuum infusion of specimens S-COR-VI-1 & 2.

with a reasonable thickness, the target value of 0.3 was selected for the stiffness ratio. Thus, 18 layers were finally used for the T/HLU and T/VI patches and the finally achieved SR values were 0.32 for the T/HLU material and 0.31 for the T/VI one. It must be noted at this point that these values of SR is quite lower than the value of $SR = 1.0$ which is suggested in the literature [6], but for pre-preg composite materials, much stiffer than the Twill

fabric.

In the case of the UD-HM/HLU patches (specimens S-COR-HLU-3 & 4), it was decided to keep the same number of layers to that of the Twill material, in order to investigate the effect of the different SR and the different patch thickness. Thus, the SikaWrap patches were also made of 18 layers, resulting in a SR of 2.6, a value much higher than the 0.32 and 0.31 of the other specimens.

As shown in Figure 1, patch edges were manufactured as tapered in order to avoid high debonding stresses. Thus the 18 layers of each patch were split in four groups, which have the same width but different length. The 5 layers of the first group had a length of 200 mm, the other 5 of the second group a length of 232 mm, the 4 layers of the third group a length of 264 mm and rest 4 of the final fourth group a 300 mm length. Thus, each group of layers covers the previous one.

2.4 Test parameters

A preloading of 30 kN was initially applied on the specimens, in order to minimize the specimen-fixtures assembly tolerances. The final loading was applied in the form of a linearly increasing tensile displacement with a rate of 0.5 mm/s. The test was terminated when the patch was no more contributing to the stiffness of the specimen and the steel part of the specimen had entered well into plasticity.

The applied force, the total specimen elongation and the longitudinal strains at various locations on the specimen were recorded during each test. In the case of the patched specimens, strains were recorded at seven locations, five on the patched side and two on the unpatched side. Strain gages SG-1 to SG-4 were placed on the patch and had a 25 mm spacing (see Figure 1). Strain gage SG-5 was placed exactly as SG-1 but on the opposite unpatched side, whereas SG-7 was placed at the exactly opposite point from SG-6. In the case of the unpatched specimens, strains were measured at SG-5, SG-6 and SG-7.

3. RESULTS AND DISCUSSION

All experimental measurements are presented in the following in the form of graphs. Figure 4 shows the global response of all specimens, in the form of the total elongation of each specimen (distance between the testing machine grips) versus the applied tensile force. Reference unpatched specimens S-COR-1 & 2 present an expected behaviour, initially responding linearly and then passing into plasticity. The entrance into plasticity is taking place for the load values shown in Table 2 (yield loads). The average yield

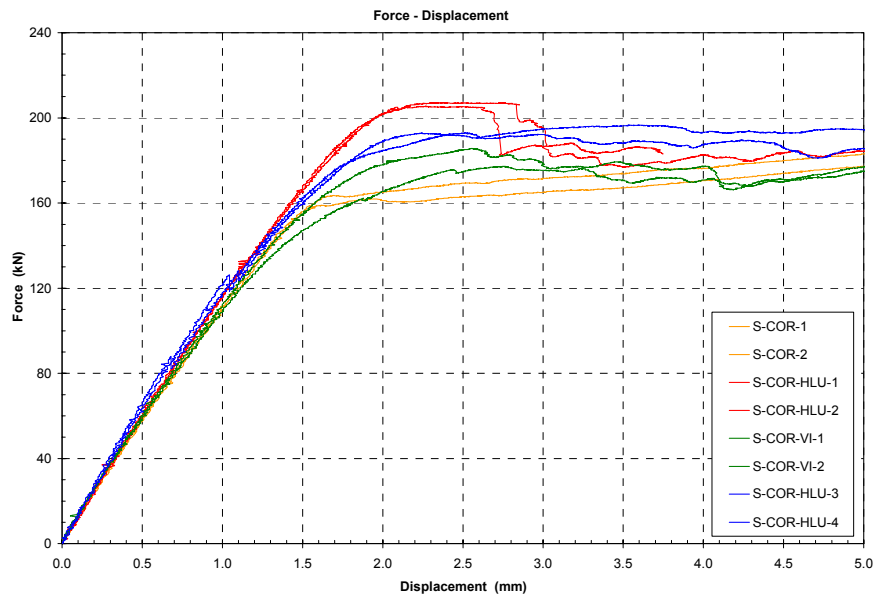


Figure 4: Specimens' elongation versus applied load.

load of the unpatched specimens is 160.6 kN, a value which is very close to the theoretically calculated one (158.3 kN) for the steel effective cross section at the corroded area ($140 \times 3.25 \text{ mm}^2$, see Table 1).

All patched specimens present in general a similar behaviour. Initially they deform elastically, with the elastic response region being greater than that of the reference unpatched specimens. This can be explained by the fact that the presence of the patch results in a decrease of the developed stresses on the steel adherent for the same applied loading, thus the specimen behaves elastically up to higher loads. After this stage, the specimens enter plasticity. In order to explain their further behaviour, additional magnitudes of the experimental measurements should be taken into account. It must be reminded at this point that the loading is applied as a linearly increasing tensile displacement, thus any change in the stiffness of a specimen results in a corresponding change of the force carried.

Figures 5 to 7 present the additional measurements needed to explain the specimens' behaviour. Figure 5 shows the variation of strain from SG-5 at the center of the back

Table 2: Failure load of all specimens.

Specimen	Patch Failure Load (kN)	Average % Difference ²
S-COR-1	158.0 ¹	-
S-COR-2	163.1 ¹	-
S-COR-HLU-1	206.9	28
S-COR-HLU-2	205.1	
S-COR-VI-1	177.2	13
S-COR-VI-2	185.5	
S-COR-HLU-3	196.5	21
S-COR-HLU-4	192.9	

¹ Yield load.

² From the average of the yield loads of reference specimens S-COR-1 and S-COR-2.

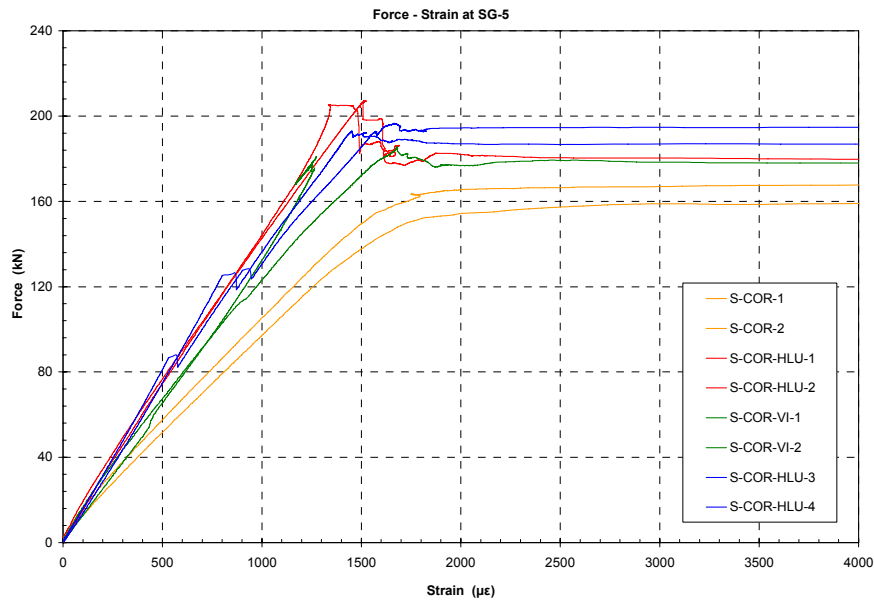


Figure 5: Strains at SG-5 versus applied load.

side of the specimen versus the applied force, whereas Figure 6 shows the variation of strains measured from SG-6 and SG-7 away from the patch, versus the applied displacement. This latter choice of applied displacement instead of applied force for the results of Figure 6 owes to the fact that in this way these specific strain curves are much more legible and informative. In addition to these results, Figure 7 presents the variation of strain measured from SG-1 at the center of the patch, versus the applied load. The experimental results of this figure determine the patch failure load of each specimen, which is the maximum load after which strains on the patch drop, that is the load value where patches stop contributing into the global specimen stiffness. The so extracted patch failure loads are cited in Table 2 and are compared to the yield loads of the reference unpatched specimens.

The behaviour of the patched specimens can be investigated by the concurrent study

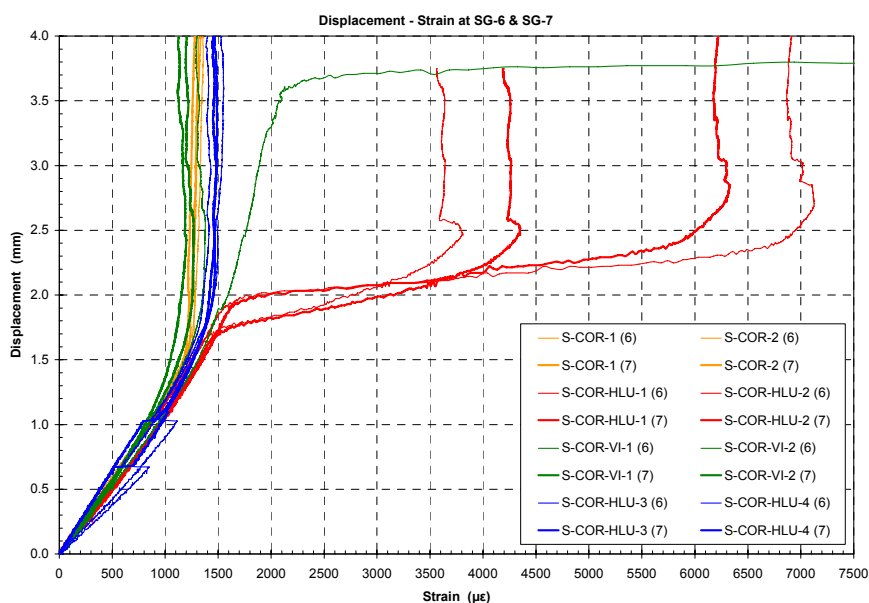


Figure 6: Strains at SG-6 and SG-7 versus applied displacement.

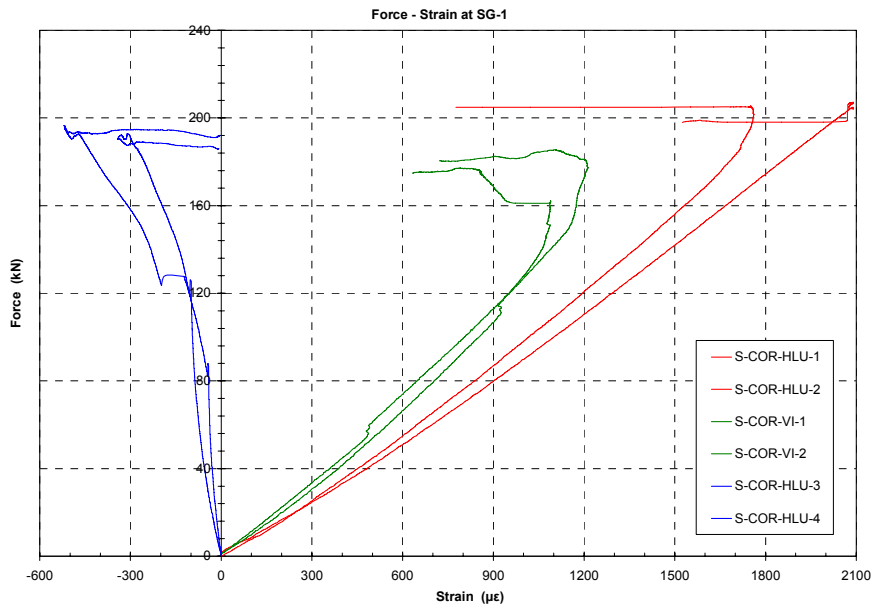


Figure 7: Strains at SG-1 versus applied load.

of Figures 4, 5, 6 and 7. Thus, for specimens S-COR-HLU-1 & 2, the strain measurements of Figure 6 indicate that, for an applied displacement of 1.7 to 1.9 mm (approximately 180 to 195 kN), these two specimens enter plasticity at the area of SG-6 and SG-7, that is away from the patched corroded region. As loading continues to increase, Figure 5 shows that the steel region exactly under the patch also enters plasticity. Simultaneously, we have debonding of the patch with a sudden drop of the applied force (see Figures 4 and 7), whereas, further up in loading, strains at SG-6 and SG-7 stop increasing (Figure 6), and plasticity is confined only under the patched corroded area of the specimen (see Figure 5). After the patch debonding, specimens S-COR-HLU-1 & 2 follow the general behaviour of the reference unpatched specimens, as expected.

Contrary to the case of the above two specimens, patch debonding of all other patched specimens was not sudden but progressive, as evidenced by the results of Figure 4. Moreover, Figures 5 and 6 show that all other specimens do not enter plasticity at SG-6 and SG-7 positions away from the patch, but at position SG-5, under the corroded patched area. The only exception is specimen S-COR-VI-1, which never enters plasticity at SG-5, but only at SG-6.

The study of Figure 4 and Table 2 reveals the clear superiority of the patched specimens against the unpatched ones, since the maximum load reached by the former before patch debonding is from 13 to 28% increased with respect to the yield load of the latter. Specimens with T/HLU patches presented a significant improvement in their performance, despite their very low SR of 0.32.

Comparing the materials used for manufacturing the patches, it is very interesting to compare first the behaviour of specimens with T/HLU patches to the behaviour of specimens with T/VI patches, which exhibit approximately the same stiffness ratio. The superiority of the HLU patches is clear, probably due to the larger quantity of resin, which leads to the achievement of a more efficient bond between the patch and the steel plate. On the contrary, in the case of the T/VI patches, it seems that the existing resin quantity was not enough for the achievement of an equally efficient bond. This

conclusion was verified by examining the bond surface of the patches after their debonding from the steel adherent. It was found that the T/HLU patches presented a well resin impregnated bond surface, contrary to the bond surface of the T/VI patches which exhibited some air voids and dry areas. The larger resin quantity of the hand laid-up patches results normally in thicker T/HLU patches. Consequently, it becomes evident that, for a low and constant SR value, it is better to use materials with lower modulus and greater thickness, instead of others which are stiffer but thinner. This conclusion is verified by corresponding numerical studies, as well as from the dynamic and the static behaviour of similar cracked specimens [9, 10].

The behaviour of the T/HLU patched specimens was better than that of the UD-HM/HLU ones, despite the fact that the latter have a much higher SR (2.6 against 0.32). This inconsistency may either owe to some air voids noted at the UD-HM/HLU patches bonding surface after their debonding, or to the greater eccentricity and to the, thus, resulting higher bending stresses, due to the excessively large thickness of these patches in comparison with the thickness of the T/HLU ones. These high bending stresses lead to an early failure of the patch-plate adhesive bond. It seems, therefore, that a large patch thickness is favourable up to a certain limit of SR, above which thicker one-side patches have a negative effect. The full explanation of this phenomenon necessitates the performance of further experimental and numerical studies. However, such inconsistencies have been also noticed in other similar experimental tests [6].

Studying the strains behaviour, Figure 5, presenting measured strains from SG-5 on the back side of the patched corroded area of the specimen, indicates from another perspective the sudden patch debonding of specimens S-COR-HLU-1 & 2 and the gradual debonding of the patches of all other specimens. After debonding, strains continue to increase up to failure, indicating that yield is taking place at the diminished cross section of the corroded area, as expected. An exception from this rule is the behaviour of specimen S-COR-VI-1, which yields up to failure in another position and, thus, strains at SG-5 remain low ($<1300 \mu\epsilon$).

This exception is clearly shown in Figure 6, presenting the strain measurements from SG-6 and SG-7, away from the patch. Strain from specimen S-COR-VI-1 is always increasing up to failure. Strains from specimens S-COR-HLU-1 & 2 indicate that temporary yield is taking place at these positions for these two specimens, whereas strains from all other specimens remain in the elastic response range ($<1600 \mu\epsilon$).

Figure 6 indicates also the extensive local bending of specimens S-COR-HLU-3 & 4 that is taking place during the elastic response phase, before gradual patch debonding starts. A comparison of the elastic strains measured at position 6 for these two specimens (thin blue lines) to those measured at position 7 (thick blue lines) reveals that the former are considerably higher than the latter. These differences owe to the local bending that is taking place at the central area of the specimens, due to the unsymmetric cross section of the one-side patched specimens. This asymmetry is much more pronounced in the case of these two specimens, due to the large thickness of the patch (12.6 mm). The one-side patch causes the development of a deflection towards the steel part of the cross section, a deflection which increases as the tensile load increases. Therefore, near the specimen edges, additional tensile strains are developed at position 6, whereas on the opposite side (position 7) a part of the tensile strains due to the tensile load is compensated by the compressive strains due to bending of the specimen.

The variation of strains from SG-2, SG-3 and SG-4 on the patch versus the applied force is similar to that from SG-1 shown in Figure 7. The first general conclusion that

can be drawn out from the variation of patch strains is that there is good repeatability of the results for the pairs of similar specimens, with the exception of S-COR-VI-1 specimen, due to its particular behaviour. The next conclusion is that specimens S-COR-HLU-3 & 4 present a different behaviour than the other four. Thus, patch strains at specimens S-COR-HLU-1 & 2 and S-COR-VI-1 & 2 are always tensile, presenting an approximately linear behaviour up to the load where patch debonding starts. However, patch strains at specimens S-COR-HLU-3 & 4 are always compressive and deviating from the linear response. This behaviour can be explained by the fact that these two specimens have a much thicker patch with a much higher SR than the others, something that results in a much more pronounced local bending due to the unsymmetric cross-section, as it was discussed before. Therefore, the free patch surface is in compression, despite the overall tensile loading.

4. CONCLUSIONS

The following conclusions can be drawn out from the present experimental study:

- In two out of the three cases investigated (S-COR-VI-1 & 2 and S-COR-HLU-3 & 4), patch failure appeared as gradual debonding from the steel adherent, accompanied by a simultaneous yield of the steel specimens, either at their corroded area or elsewhere. In the third case (S-COR-HLU-1 & 2), yield at the corroded area of the steel adherent appeared first, soon followed by a sudden patch debonding.
- The maximum load reached by the patched specimens before patch debonding is increased with respect to the yield load of the reference unpatched specimens. This increase varies from 13 up to 28%. Specimens with patches made of Twill carbon fabric using the hand lay-up method exhibited best performance, despite their low SR of 0.32.
- In order to achieve a specific stiffness ratio for the patched structure, it is better to use patch materials with lower elastic modulus and greater thickness instead of others which are stiffer but thinner.
- It was experimentally verified that the thicker the patch is, the more intense is bending caused by the unsymmetric cross section of the one-side patched structure.
- The worse than expected behaviour of the high stiffness ratio specimens with UD-HM/HLU patches necessitates further experimental and numerical study. However, it appears that the selection of the most proper value for the SR must be performed taking always into account the resulting patch thickness, in order not to create intense bending behaviour, that results in early patch debonding. In parallel, one must always also consider the strength of the adhesive between the patch and the steel substrate, since the selection of a patch that carries less load (and therefore does not unload as much the steel structure) might be preferable from a stronger patch which loads more the adhesive and causes its early failure.
- Patch strains remain constant in the central area of the patch. The variation of these strains along the patch indicates that a longer patch might be more effective in the present application.
- The portion of the applied loading that is carried by the patch is significant and slightly decreases as the applied loading increases. This fact indicates that a stronger steel to patch bond would result in a much more efficient reinforcement of the corroded steel specimens.

All experimental measurements performed within the framework of this study can be used for the validation of corresponding finite element models.

ACKNOWLEDGMENTS

The authors gratefully acknowledge the support of research project PYTHAGORAS II, which is co-funded by the European Social Fund (75%) and National Resources (25%). Thanks are also expressed to Elefsis Shipyards S.A. for supplying the steel plates and to SIKA Hellas S.A. for supplying the SIKA carbon/epoxy composite system. The authors also acknowledge the support of Messrs A. Markoulis, M. Nounos and H. Xanthis for participating in the experimental activities.

REFERENCES

- 1- Baker, A.A., Jones, R., *Bonded Repair of Aircraft Structures*, Kluwer Academic Publishers, 1988.
- 2- Baker, A., “Bonded Composite Repair of Fatigue-Cracked Primary Aircraft Structure”, *Composite Structures*, 1999; 47: 431-443.
- 3- Okafor, A.C., Bhogapurapu, H., “Design and Analysis of Adhesively Bonded Thick Composite Patch Repair of Corrosion Grind-out and Cracks on 2024 T3 Clad Aluminum Aging Aircraft Structures”, *Composite Structures*, 2006; 76: 138-150.
- 4- Phelps, B.P., “Bonded Repairs to RAN FFG Superstructure – Strain Gauge Data Analysis”, Department of Defence of Australia, *DSTO Report DSTO-RR-0046*, 1995.
- 5- Grabovac, I., “Bonded Composite Solution to Ship Reinforcement”, *Composites: Part A*, 2003; 34: 847-854.
- 6- Dalzel-Job, J., Sumpter, J.D.G., Livingstone, F., “Composite Patch Repair of Steel Ships”, *Proceedings of Advanced Marine Materials, Technology and Applications Conference, RINA*, London, 2003.
- 7- Turton, T.J., Dalzel-Job, J., Livingstone, F., “Oil Platforms, Destroyers and Frigates – Case Studies of QinetiQ’s Marine Composite Patch Repairs”, *Composites: Part A*, 2005; 36: 1066-1072.
- 8- Tsouvalis, N.G., Mirisiotis, L.S., “Experimental Investigation of the Static Behaviour of a Hole Drilled Steel Plate Reinforced with a Composite Patch”, *Strain*, 2008; 44: 133-140.
- 9- Tsouvalis, N.G., Mirisiotis, L.S., Papazoglou, V.J., “Fatigue Behaviour of Composite Patch Reinforced Steel Plates”, *Proceedings of the International Conference on Structural Analysis of Advanced Materials (ICSAM 2007)*, Patras, Greece, 2007.
- 10- Mirisiotis, L.S., Tsouvalis, N.G., “Experimental Investigation of a Composite Patch Reinforced Cracked Steel Plate in Static Loading”, *Proceedings of the 9th International Conference on Fast Sea Transportation (FAST 2007)*, Shanghai, China, 2007.
- 11- Mirisiotis, L.S., Tsouvalis, N.G. and Tsiourva, T.E., “Experimental Investigation of the Static Tensile Behaviour of Corroded Steel Plates Reinforced with Composite Patches”, National Technical University of Athens, Shipbuilding Technology Laboratory, Report No. STL-238-F-07, May 2007.